APPLIED PHYSICS LETTERS **90**, 183516 (2007)

40% efficient metamorphic GaInP/GaInAs/Ge multijunction solar cells

R. R. King,[a] D. C. Law, K. M. Edmondson, C. M. Fetzer, G. S. Kinsey, H. Yoon, R. A. Sherif, and N. H. Karam

Spectrolab, Inc., 12500 Gladstone Ave., Sylmar, California 91342

(Received 8 March 2007; accepted 3 April 2007; published online 4 May 2007)

An efficiency of 40.7% was measured and independently confirmed for a metamorphic three-junction GaInP/GaInAs/Ge cell under the standard spectrum for terrestrial concentrator solar cells at 240 suns (24.0 W/cm^2, AM1.5D, low aerosol optical depth, 25 °C). This is the initial demonstration of a solar cell with over 40% efficiency, and is the highest solar conversion efficiency yet achieved for any type of photovoltaic device. Lattice-matched concentrator cells have now reached 40.1% efficiency. Electron-hole recombination mechanisms are analyzed in metamorphic $Ga_xIn_{1-x}As$ and $Ga_xIn_{1-x}P$ materials, and fundamental power losses are quantified to identify paths to still higher efficiencies. © *2007 American Institute of Physics*. [DOI: 10.1063/1.2734507]

Light emitted by the sun and falling on Earth is one of the most plentiful energy resources on the planet. Over 1.5×10^{22} J (15 000 EJ) of solar energy reach Earth everyday, compared to a daily energy consumption of approximately 1.3 EJ by human activity.[1] However, solar radiation is a broadly distributed energy resource both in terms of geographic distance, requiring large, expensive collectors, and in terms of its wide range of wavelengths. Multijunction III–V solar cells for terrestrial concentrator applications have attracted increasing attention in recent years for their very high conversion efficiencies, allowing dramatic reduction in the balance-of-system cost for photovoltaic electricity generation. Such multijunction cells use multiple subcell band gaps to divide the broad solar spectrum into smaller sections, each of which can be converted to electricity more efficiently, allowing cell efficiencies beyond the Shockley-Queisser theoretical limit for single-junction cells[2] to be achieved in practice.

Metamorphic, or lattice-mismatched, semiconductors provide an unprecedented degree of freedom in solar cell design, by providing flexibility in band gap selection, unconstrained by the lattice constant of common substrates such as Ge, GaAs, Si, InP, etc. Other devices can also benefit from these materials, such as heterojunction bipolar transistors, 1.3 and 1.55 μm photodetectors and lasers, and InP-on-GaAs and GaAs-on-Si devices in general. Many research studies have investigated the promise of metamorphic materials for solar cells,[3–11] often citing 40% conversion efficiency as a possible goal. This letter reports on three-junction metamorphic and lattice-matched cells that have now surpassed the 40% efficiency milestone.

Figure 1 plots isoefficiency contours for three-junction terrestrial solar cells at 240 suns concentration, as a function of the top (subcell 1) and middle (subcell 2) band gaps. These are ideal efficiencies, calculated based on the fundamental mechanism of radiative recombination, the AM1.5D terrestrial solar spectrum, and the *I-V* characteristics of each subcell.[11] Band gap combinations of GaInAs and GaInP at the same lattice constant are plotted, for GaInP with a disordered group-III sublattice (high E_{g1}) and for ordered GaInP (low E_{g1}). The record 40.7% efficiency metamorphic and 40.1% efficiency lattice-matched three-junction cells described in this letter are plotted, showing the advantage of the metamorphic cell design in practice now, as well as in theory. Decreasing the band gap of the top two subcells, e.g., by raising the indium content, brings the three-junction cell design closer to the peak efficiency. Similar analyses can be carried out for terrestrial concentrator cells with four and more junctions with over 58% theoretical efficiency.[11]

Fundamental loss mechanisms in metamorphic (MM) and lattice-matched (LM) three-junction GaInP/GaInAs/Ge solar cells are plotted in Fig. 2. Unabsorbed photons ($h\nu < E_{g3}$) cause the same loss in the MM and LM cases. Carrier thermalization losses for subcells 1 and 2 ($h\nu > E_{g1}$ and $h\nu > E_{g2}$) are lower for LM cells, due to their higher band gaps, but subcell 3 thermalization losses ($h\nu > E_{g3}$) are smaller in the MM case, due to lower average photon energy reaching the Ge subcell. Losses from the band gap-voltage offset $(E_g/q)-V_{oc}$ due to radiative recombination decline steadily with increasing light intensity as the electron and

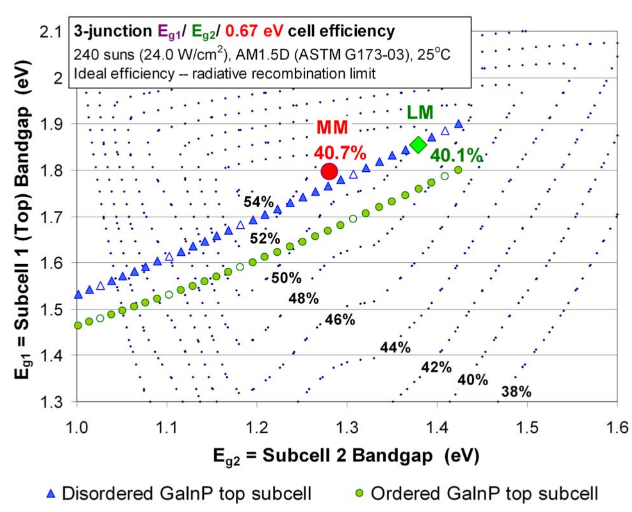

FIG. 1. (Color online) Calculated contours of ideal three-junction solar cell efficiency as a function of top and middle subcell band gaps, E_{g1} and E_{g2}. Measured efficiencies and E_{g1}, E_{g2} combinations are shown for the record efficiency 40.7% MM and 40.1% LM cells described in the text. The band gaps in the metamorphic GaInP/GaInAs system are plotted for disordered and ordered group-III sublattices in the GaInP subcell.

[a]Electronic mail: rking@spectrolab.com

0003-6951/2007/90(18)/183516/3/$23.00

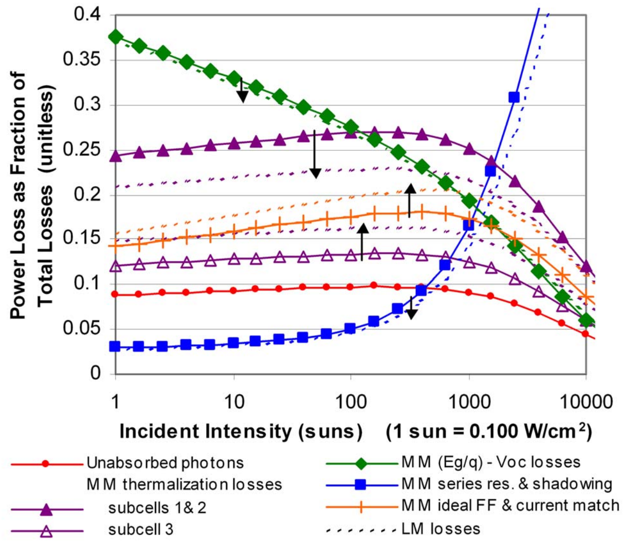

FIG. 2. (Color online) Loss mechanisms in metamorphic $Ga_{0.44}In_{0.56}P/Ga_{0.92}In_{0.08}As/Ge$ and lattice-matched $Ga_{0.50}In_{0.50}P/Ga_{0.99}In_{0.01}As/Ge$ three-junction terrestrial solar cells as a function of incident intensity of sunlight.

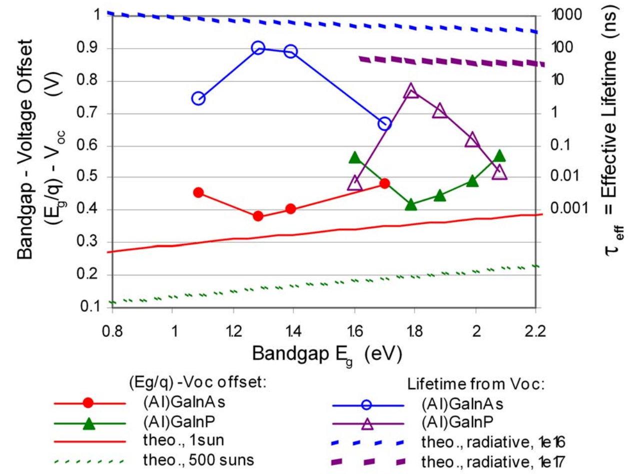

FIG. 3. (Color online) Measured band gap-voltage offset for a range of LM and MM subcell materials and bandgaps at 1 sun. Comparison to theory gives a measure of the SRH recombination present. The effective lifetime, an upper limit on the bulk lifetime, is derived from the cell measurements.

hole quasi-Fermi levels approach their respective band edges in each subcell. The high efficiency of the MM design results largely from lower current match losses, since there is less excess photogenerated current density in the Ge bottom cell, due to the lower band gaps of the MM subcells. Metal grid shadowing and I^2R resistive power losses are greater for MM cells because of their higher currents, but the MM design retains its overall efficiency advantage.

The central challenge tempering the band gap flexibility offered by metamorphic materials is that lattice-mismatched growth typically causes crystal dislocations, introducing energy levels in the band gap which mediate Shockley-Read-Hall (SRH) recombination. A composition-graded buffer is used to accommodate misfit and threading dislocations to the greatest extent possible. The active metamorphic (meaning *changed form*) device layers can then be grown relaxed with low dislocation density at the new lattice constant. The single- and three-junction experimental cells here are grown on 100 mm Ge substrate wafers by metal-organic vapor-phase epitaxy, in production-scale reactors. The nontextured, p-type Ge substrate forms the third subcell of the three-junction cells, by virtue of an n-type diffused emitter formed during growth of the upper epitaxial layers.

In Fig. 3, the band gap-voltage offset $(E_g/q)-V_{oc} \equiv W_{oc}$ at 1 sun is plotted for a wide range of band gaps in LM and MM (Al)GaInP and (Al)GaInAs subcells. This band gap-voltage offset W_{oc} varies only slowly over a wide range of band gaps, and it can be helpful simplifying approximation to treat it as a constant to first order, e.g., at ~ 0.4 V at 1 sun. For a solar cell limited by radiative recombination in the base, for example,

$$V_{oc} = \frac{kT}{q}\ln\left(\frac{J_{ph}}{qwBn_i^2}\right) = \frac{E_g}{q} - \frac{kT}{q}\ln\left(\frac{qwBN_CN_V}{J_{ph}}\right), \qquad (1)$$

for photogenerated current density J_{ph}, radiative recombination coefficient B, and solar cell base thickness w, so that the band gap dependence of the offset W_{oc} is only a slowly varying natural log function. Deviation from the radiative limit of W_{oc} is a good indicator of the amount of the nonideal mechanism of SRH recombination that is present and, thus, of the semiconductor crystal quality.

In general,

$$pn = n_i^2 e^{qV/kT} = N_CN_Ve^{-q((E_g/q)-V)/kT} = N_CN_Ve^{-qW/kT}, \qquad (2)$$

where $W \equiv (E_g/q)-V$. For low-level injection in a p-type solar cell base with doping N_A, the effective minority-carrier lifetime τ_{eff}, an upper limit on the bulk lifetime, is

$$\tau_{eff} = \frac{qw}{J_{ph}}\frac{N_CN_V}{N_A}e^{-qW_{oc}/kT} \qquad (3)$$

in the long diffusion length (narrow-base) limit.

In Fig. 3, LM 1.4 eV and MM 1.3 eV GaInAs, and LM 1.9 eV and MM 1.8 eV GaInP, have the lowest band gap-voltage offsets and highest τ_{eff}, approaching the theoretical limits from radiative recombination. Band gap-voltage offsets of 0.42 and 0.38 V, corresponding to effective minority-carrier lifetimes of 5 and 100 ns, were measured in p-type metamorphic $Ga_{0.44}In_{0.56}P$ and $Ga_{0.92}In_{0.08}As$, respectively, with doping in the $10^{16}-10^{17}$ cm^{-3} range. Relatively low W_{oc} and correspondingly long τ_{eff} are maintained even for high 1.6% lattice mismatch to the Ge growth substrate in metamorphic $Ga_{0.77}In_{0.23}As$, with band gap of 1.1 eV.

A capture cross-sectional width t_n can be defined that relates the areal density N_{disloc} of line dislocations that typically form in metamorphic materials to the lifetime τ_{eff}, such that $\tau_{eff}=1/(N_{disloc}v_{th}t_n)$, where $v_{th}=(3kT/m^*)^{1/2}$ is the thermal velocity of minority electrons. From cathodoluminescence and plan-view transmission electron microscopy, an average value of $N_{disloc} \approx 8 \times 10^6$ cm^{-2} is measured for $Ga_{0.77}In_{0.23}As$ on Ge (including both threading dislocation segments typically in each defect complex). Using $\tau_{eff}=2.8$ ns from measured $(E_g/q)-V_{oc}$ of $Ga_{0.77}In_{0.23}As$ cells, and $v_{th}=4.5\times10^7$ cm/s, yields an effective cross-sectional width t_n of the dislocations of $\sim 1\times10^{-6}$ cm for purposes of calculating recombination. One can also assign an approximate capture cross section σ_n to each incompletely bound atom along the line dislocations, correlating volumetric trap density N_t to τ_{eff}. For two atoms with one dangling bond each per unit cell with side a, and line dislocations

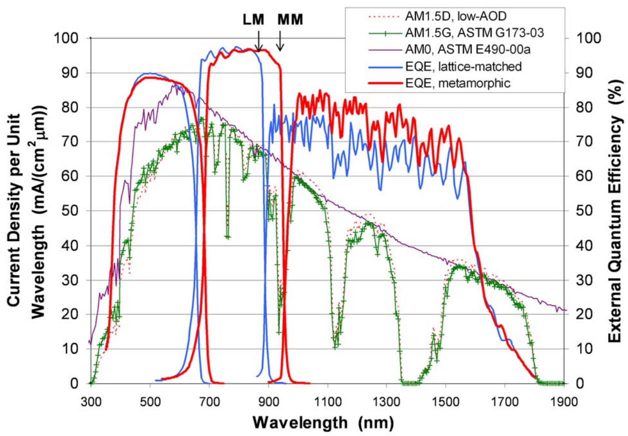

FIG. 4. (Color online) External quantum efficiency for GaInP, GaInAs, and Ge subcells in MM and LM three-junction cells, and the space and terrestrial solar spectra.

typically running along the energetically preferred ⟨110⟩ directions, $N_t=(2/a)N_{\mathrm{disloc}}$, and $\sigma_n=t_n a/2=a/(2N_{\mathrm{disloc}}v_{\mathrm{th}}\tau_{\mathrm{eff}})\approx 3\times 10^{-14}\ \mathrm{cm}^2$.

In Fig. 4, measured external quantum efficiencies are shown for the GaInP, GaInAs, and Ge subcells in MM and LM three-junction cells, superimposed on the air mass zero and terrestrial solar spectra. The downward shift in band gap in the upper two MM subcells is evident, allowing the higher voltage upper subcells to use a larger part of the solar spectrum. The long wavelength response of the MM $Ga_{0.44}In_{0.56}P$ and $Ga_{0.92}In_{0.08}As$ subcells can be seen to be high near the band edge, reflecting the long lifetimes and diffusion lengths in these metamorphic materials.

Metamorphic three-junction $Ga_{0.44}In_{0.56}P/Ga_{0.92}In_{0.08}As/Ge$ terrestrial concentrator solar cells with a graded buffer structure and low threading dislocation density were grown and fabricated under a wide range of experimental conditions. Figure 5 plots the measured illuminated *I-V* curve for a record efficiency 40.7% metamorphic GaInP/GaInAs/Ge three-junction cell at 240 suns, under the standard spectrum for terrestrial concentrator solar cells (AM1.5D, low aerosol optical depth, 24.0 W/cm^2, 25 °C).

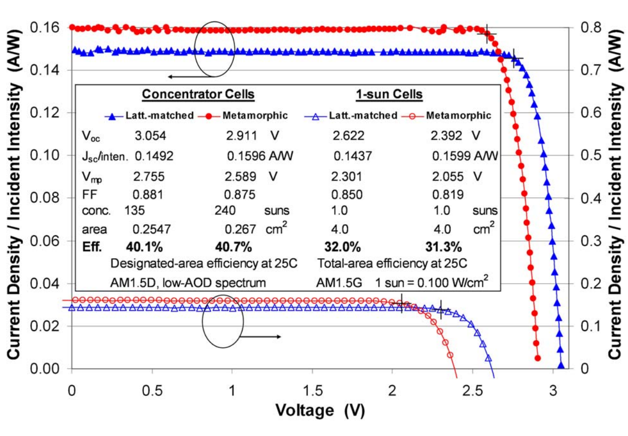

FIG. 5. (Color online) Measured illuminated *I-V* characteristics of record efficiency 40.7% metamorphic and 40.1% lattice-matched three-junction solar cells under the concentrated terrestrial solar spectrum, and 31.3% MM and 32.0% LM 1 sun cells. These measurements are independently verified by the National Renewable Energy Laboratory (NREL).

This is the initial demonstration of a solar cell with over 40% efficiency, and is the highest solar conversion efficiency yet achieved for any type of photovoltaic device. A lattice-matched three-junction cell has now also achieved over 40% efficiency, with 40.1% measured at 135 suns (AM1.5D, low-AOD, 13.5 W/cm^2, 25 °C). This record efficiency lattice-matched cell, and earlier MM and LM record 1 sun cell efficiencies are also plotted in Fig. 5. The total measurement uncertainty in efficiency is estimated to be 2.4% absolute. Both the 40.7% metamorphic and 40.1% lattice-matched cells surpass the earlier record efficiencies of 39.3% for a MM cell[11] and 39.0% for a LM cell.[9] These efficiency measurements have been verified by the independent solar cell test facility at the National Renewable Energy Laboratory (NREL).

It is interesting to note in Fig. 5 that the 1 sun cells have measured efficiency above the Shockley-Queisser limit efficiency of 30% for a single-band gap device at 1 sun,[2] and the concentrator cells are above the theoretical limit of 37% for single-band gap cells at 1000 suns,[12] due to the multijunction structure of these cells. Experimental multijunction cell architectures, using features such as metamorphic materials, four or more junctions, and other design approaches have the potential to increase practical terrestrial concentrator cell efficiencies over 45%, or even to 50%.

The authors would like to thank Robert McConnell, Martha Symko-Davies, Fannie Posey-Eddy, Keith Emery, James Kiehl, Tom Moriarty, Manuel Romero, and the entire multijunction solar cell team at Spectrolab. This work was supported in part by the NREL High Performance PV program (ZAT-4-33624-12), and by Spectrolab, Inc.

[1]Energy Information Administration, International Energy Annual 2004, released May–July 2006, http://www.eia.doe.gov/iea/overview.html
[2]W. Shockley and H. J. Queisser, J. Appl. Phys. **32**, 510 (1961).
[3]M. Yamaguchi and C. Amano, J. Appl. Phys. **58**, 3601 (1985).
[4]R. R. King, M. Haddad, T. Isshiki, P. Colter, J. Ermer, H. Yoon, D. E. Joslin, and N. H. Karam, Proceedings of the 28th IEEE Photovoltaic (PV) Specialists Conference, (IEEE, Piscataway, NJ, 2000), p. 982.
[5]F. Dimroth, U. Schubert, and A. W. Bett, IEEE Electron Device Lett. **21**, 209 (2000).
[6]C. L. Andre, A. Khan, M. Gonzalez, M. K. Hudait, E. A. Fitzgerald, J. A. Carlin, M. T. Currie, C. W. Leitz, T. A. Langdo, E. B. Clark, D. M. Wilt, and S. A. Ringel, Proceedings of the 29th IEEE PV Specialists Conference, (IEEE, Piscataway, NJ, 2002), p. 1043.
[7]T. Takamoto, T. Agui, K. Kamimura, M. Kaneiwa, M. Imaizumi, S. Matsuda, and M. Yamaguchi, Proceedings of the Third World Conference on PV Energy Conversion, (Arisumi, Japan, 2003), p. 581.
[8]M. W. Wanlass, S. P. Ahrenkiel, R. K. Ahrenkiel, D. S. Albin, J. J. Carapella, A. Duda, J. F. Geisz, Sarah Kurtz, T. Moriarty, R. J. Wehrer, and B. Wernsman, Proceedings of the 31st IEEE PV Specialists Conference (IEEE, Piscataway, NJ, 2005), p. 530.
[9]R. R. King, D. C. Law, C. M. Fetzer, R. A. Sherif, K. M. Edmondson, S. Kurtz, G. S. Kinsey, H. L. Cotal, D. D. Krut, J. H. Ermer, and N. H. Karam, Proceedings of the 20th European PV Solar Energy Conference, Barcelona, Spain, (WIP-Renewable Energies, Munich, 2005), p. 118.
[10]R. R. King, D. C. Law, K. M. Edmondson, C. M. Fetzer, R. A. Sherif, G. S. Kinsey, D. D. Krut, H. L. Cotal, and N. H. Karam, Proceedings of the Fourth World Conference on PV Energy Conversion, Waikoloa, Hawaii, (IEEE, Piscataway, NJ, 2006), p. 760.
[11]R. R. King, R. A. Sherif, D. C. Law, J. T. Yen, M. Haddad, C. M. Fetzer, K. M. Edmondson, G. S. Kinsey, H. Yoon, M. Joshi, S. Mesropian, H. L. Cotal, D. D. Krut, J. H. Ermer, and N. H. Karam, Proceedings of the 21st European PV Solar Energy Conference, Dresden, Germany, (WIP-Renewable Energies, Munich, 2005), p. 124.
[12]C. H. Henry, J. Appl. Phys. **51**, 4494 (1980).